Cellular and Molecular Life Sciences (2019) 76:4551–4568
https://doi.org/10.1007/s00018-019-03127-z

ORIGINAL ARTICLE

CNDP1 knockout in zebrafish alters the amino acid metabolism, restrains weight gain, but does not protect from diabetic complications

Felix Schmöhl[1] · Verena Peters[2] · Claus Peter Schmitt[2] · Gernot Poschet[3] · Michael Büttner[3] · Xiaogang Li[1] · Tim Weigand[2] · Tanja Poth[4] · Nadine Volk[5] · Jakob Morgenstern[6] · Thomas Fleming[6] · Peter P. Nawroth[6,7,8] · Jens Kroll[1]

Received: 7 December 2018 / Revised: 22 April 2019 / Accepted: 30 April 2019 / Published online: 9 May 2019

Abstract

The gene *CNDP1* was associated with the development of diabetic nephropathy. Its enzyme carnosinase 1 (CN1) primarily hydrolyzes the histidine-containing dipeptide carnosine but other organ and metabolic functions are mainly unknown. In our study we generated *CNDP1* knockout zebrafish, which showed strongly decreased CN1 activity and increased intracellular carnosine levels. Vasculature and kidneys of *CNDP1*$^{-/-}$ zebrafish were not affected, except for a transient glomerular alteration. Amino acid profiling showed a decrease of certain amino acids in *CNDP1*$^{-/-}$ zebrafish, suggesting a specific function for CN1 in the amino acid metabolisms. Indeed, we identified a CN1 activity for Ala–His and Ser–His. Under diabetic conditions increased carnosine levels in *CNDP1*$^{-/-}$ embryos could not protect from respective organ alterations. Although, weight gain through overfeeding was restrained by *CNDP1* loss. Together, zebrafish exhibits CN1 functions, while *CNDP1* knockout alters the amino acid metabolism, attenuates weight gain but cannot protect organs from diabetic complications.

Keywords Amino acids · Carnosinase1 · Carnosine · CRISPR/Cas · Diabetes · Diabetic nephropathy · Metabolism · Mutagenesis · Zebrafish

Abbreviations

CARNS1	Carnosine synthase
CN1	Carnosinase1 (enzyme)
CNDP1	Carnosinase1 (gene)
CN2	Carnosinase2 (enzyme)
CNDP2	Carnosinase2 (gene)
DN	Diabetic nephropathy
MG	Methylglyoxal
pdx1	Pancreas and duodenal homeobox 1

Introduction

Worldwide diabetes mellitus is one of the leading metabolic diseases with a continuously increasing number of patients [1]. As a consequence thereof, diabetic patients carry the risk to develop diabetic late complications, such as diabetic nephropathy (DN), diabetic retinopathy and diabetic neuropathy. DN evolved to be the most frequent cause of end-stage renal kidney disease in most countries [2]. A risk factor for diabetic patients to develop DN is their genetic profile. In meta-analysis studies various genes were identified to be associated with the development of DN [3]. In a subgroup analysis, the gene for carnosinase1 (*CNDP1*) was identified as a factor to increase susceptibility for DN in type 2 diabetic patients [4]. Carnosinases are dipeptidases that are members of the M20/M28 metalloproteases family, which cleave histidine-containing dipeptides [5]. So far, two forms of carnosinase enzymes are identified; one is the serum carnosinase, CN1 (EC 3.4.13.20), the other the tissue or cytosolic nonspecific carnosinase, CN2 (EC 3.4.13.18) [6–8]. CN1 cleaves specifically carnosine, anserine and homocarnosine, whereas

Electronic supplementary material The online version of this article (https://doi.org/10.1007/s00018-019-03127-z) contains supplementary material, which is available to authorized users.

Felix Schmöhl and Verena Peters contributed equally.

✉ Jens Kroll
jens.kroll@medma.uni-heidelberg.de

Extended author information available on the last page of the article

CN2 is not limited to histidine-containing dipeptides, degrades carnosine just under more alkaline conditions and does not degrade homocarnosine [7, 9]. Carnosine (β-alanyl-L-histidine) is synthesized by carnosine synthase (CARNS, EC 6.3.2.11) from β-alanine and L-histidine and exerts a variety of beneficial functions [10, 11]. This includes scavenging of reactive carbonyls as mediators of diabetic organ damage [12, 13], inhibition of glycation [14] and protection from oxidative stress [15]. Importantly, carnosine acts as a sensitizer for insulin secretion and glucose metabolism [16–18] because administration of carnosine to diabetic mice improved blood glucose levels, increased insulin, reduced albuminuria and vascular permeability and restored glomerular ultrastructure [18, 19].

Considering these positive actions of carnosine on organ function, the degradation of carnosine by CN1 appears to be an unsolved problem and CN1 deficient animal models, which may help to explain this, do not exist. Thus, the physiological and pathophysiological function of CN1 remained unknown thus far. Under diabetic conditions, CN1 activity is increased which can at least be partially induced via post-translational modification by reactive metabolites and leads to an increased cleavage of its protective substrate carnosine [20]. Interestingly a homozygote allelic variant ("*CNDP1* Mannheim allele") of this gene was discovered, coding for a leucine repeat, which causes lower serum carnosinase levels and was more common in the absence of DN [21].

The carnosine-carnosinase system is evolutionary highly conserved, but generally found in vertebrates [5]. In zebrafish (*Danio rerio*), two carnosinase-like genes can be identified based on their sequences. These genes are located on two different chromosomes, which is different to mouse and human where *CNDP1* and *CNDP2* are in close proximity to each other on one chromosome. One of the genes in zebrafish is annotated as *CNDP2* (ENSDARG00000003931). The second gene is found under the annotation ENSDARG00000069583 and was named *CNDP1* until reannotation of the gene number due to changed Ensemble naming policy for orthologue genes. However, it has not been reported if the enzyme resembling CN1 in zebrafish can degrade carnosine or other dipeptides. Recently, carnosine-like peptides were identified in zebrafish embryos and adults [22] and were located in eyes and neuronal areas for olfactory sensation, suggesting a function in visual and olfactory physiology. Together, the available data have reported the existence of the carnosine−carnosinase system in zebrafish but its function in organ development and disease processes remained unclear. Besides the recent description of carnostatine as a selective CN1 inhibitor [23], genetic loss of function animals for *CNDP1* are missing. However, in this study carnostatine was not tested on physiological and pathophysiological organ functions and it therefore remained unknown, what are the functional consequences of a knockdown or knockout of *CNDP1* in an animal model.

Thus, the aim of the study was to generate the first *CNDP1* knock out animal model. Subsequently, we aimed to provide a detailed characterization of organ development and function in *CNDP1* knockout zebrafish under physiological conditions as well as to address the question if the permanent loss of CN1 leads to impairing effects under disease conditions, specifically focusing on the development of late diabetic complications. We used zebrafish as a model in diabetic late complications research, because of its advantages in imaging due to the transparency of zebrafish embryos, easy genetic manipulation and characterized diabetic pathologies, giving excellent opportunities to analyze organs under diabetic conditions and accompanying metabolic alterations [24, 25]. To the best of our knowledge this study represents the first characterization of a *CNDP1* knockout organism, showing that the loss of carnosinase 1 does not impair organ development and function. However, *CNDP1* knock out zebrafish showed metabolic alterations of their amino acid metabolism.

Materials and methods

Zebrafish lines and husbandry

All experimental procedures on animals were approved by the local government authority, Regierungspräsidium Karlsruhe (license no.: 35-9185.81/G-98/15) and carried out in accordance with the approved guidelines. Embryos of the *Tg*(*wt1b:EGFP*) [26] and *Tg*(*fli1:EGFP*) [27] line were raised and staged as described according to hours post-fertilization (hpf) [28]. Embryos/larvae were kept in egg water with 5–10% methylene blue at 28.5 °C with 0.003% PTU to suppress pigmentation. Adult zebrafish were kept under 13 h light-11 h dark cycle and fed with living shrimps and fish flake food.

Inhibitors and reagents

Proteinase K (10 mg/ml stock) was utilized for embryo digestion and to finish the linearization of plasmids (Roche Recombinant PCR grade). Methylglyoxal (Sigma Aldrich) was used for embryo incubation. 0.003% 1-phenyl-2-thiourea (PTU) (Sigma) was always added to the egg water to suppress pigmentation. Texas-Red™ tagged 70 kDa dextran (Molecular Probes, Life Technologies) was used for renal functional assay [29].

Morpholinos and morpholino injection

SB-*pdx1*-Mo: 5′-GATAGTAATGCTCTTCCCGATTCA T-3′; targets the zebrafish *pdx1* translation start site. Sequence of the control-MO: 5′-CCTCTTACCTCAGTT ACAATTTATA-3′ [30] (GENE TOOLS, LLC). Pdx1 and control morpholinos were diluted to 6 µg/µl in 0.1 M KCl. One nanoliter of morpholino was injected into the yolk sack of one-cell or two-cell stage embryos [29].

Protein sequence alignment

The amino acid sequences of the CN1 proteins from zebrafish (X1WHB9_DANRE), human (CNDP1_ HUMAN) and mouse (CNDP1_MOUSE) were accessed from the UniProt Database (http://www.uniprot.org/). For the comparison, the genes were selected and aligned with the UniProt-own alignment tool (http://www.uniprot.org/align/).

Zebrafish embryo collection and preparation of kidney and brain tissue for CN1 activity assay and carnosine/anserine determination

Zebrafish embryos were anesthetized with 0.003% tricaine, collected and directly frozen in liquid nitrogen. For organ preparation adult zebrafish were euthanized with tricaine of a concentration of 0.31 mg/ml until the operculum movement stopped entirely. The fish were decapitated behind the operculum and the head was transferred into ice cold 1 × PBS. To obtain the brain, the skull was opened and all nerve connections were detached with tweezers. For preparation of the kidney, the body was cut open and transferred to ice cold 1 × PBS to remove internal organs and expose the kidney, which was isolated quickly using tweezers. Both organs were immediately frozen in liquid nitrogen after isolation.

Carnosinase activity

CN1 activity was assayed according to the method described by Teufel and co-workers [7]. Briefly, the reaction was initiated by addition of the histidine-containing dipeptides (carnosine, serine–histidine, alanine–histidine and histidine–alanine) to homogenized embryos or tissue at pH of 7. The reaction was stopped after defined periods by adding 1% trichloracetic acid (final concentration in the test 0.3%). Liberated histidine was derivatized by adding *o*-phthaldialdehyde (OPA) and fluorescence was read using a MicroTek late reader (λ_{Exc} 360 nm; λ_{Exc} 460 nm).

For the validation of our *CNDP1* knockout we used the brains of adult animals, because the CN1 activity in this tissue is higher so that we could display the loss of the enzyme clearer.

Anserine and carnosine concentrations

The detection of anserine and carnosine was measured fluorometrically using high-performance liquid chromatography as previously described [31]. Frozen Zebrafish embryos or tissue was homogenized in cold buffer containing 20 mM HEPES, 1 mM ethylene glycol-tetra-acetic acid (EGTA), 210 mM mannitol and 70 mM sucrose per gram tissue, pH 7.2. The homogenate was centrifuged at 1500 × *g* for 5 min at 4 °C, and the supernatant was kept at − 80 °C until analysis. The homogenate was diluted with sulfosalicylic acid to precipitate the proteins. After the samples were derivatized using carbazole-9-carbonyl chloride, they underwent liquid chromatography and quantification using fluorescence. The retention time of each component was determined by spiking the sample with purified carnosine or anserine.

CRISPR/Cas9 zebrafish mutant generation

The CRISPR target site for *CNDP1* was identified and selected using ZiFiT Targeter 4.1 (http://zifit.partners.org/ZiFiT/ChoiceMenu.aspx) for CRISPR/Cas Nucleases. The CRISPR target site is displayed in Fig. 2a (*CNDP1* resembles the gene with Gene ID ENSDARG00000069583). Cndp1-CRISPR-for#1 'TAGGACGTCCAGCCCGCCAAGA', was synthesized by Sigma Aldrich. Oligonucleotides were cloned into the pT7-gRNA plasmid (Addgene). *Bam*HI-HF (Biolabs) was used for linearization. Cas9 mRNA was synthesized from pT3TS plasmid (Addgene) [32] after linearizing with *Xba*I (Biolabs). Plasmids were purified with a PCR purification kit (Qiagen). CRISPR gRNA in vitro transcription was done by T7 MEGAshortscript kit and mMESSAGE MACHINE kit for Cas9 mRNA (Invitrogen). Purification of RNA after TURBO DNAse treatment was done with the MiRNeasy Mini (gRNA) and RNeasy Mini (Cas9 mRNA) kits (Qiagen). *CNDP1* gRNA and Cas9 mRNA was diluted to 150 pg/nl in 0.1 M KCl and mixed. One nanoliter of the RNA mixture was injected directly into the first cell of one-cell embryos. To identify mutant animals, genomic DNA was extracted from embryos or fin clips of adult animals by proteinase K treatment. Afterwards gene specific PCR was done (Primers: Cndp1#1_Genot-forward 'TGTGTGTGTCTCCTTCAGCT', Cndp1#1_Genot-reverse 'AAACTCTTGGCGGGCTGGACGT') and purified, followed by Sanger sequencing, using the forward primer.

Preparation of retinal vasculature

Adult zebrafish were euthanized, decapitated and heads fixed in 4% PFA/PBS over night at 4 °C. The preparation of zebrafish retinas was done as previously described [33].

Histology

Before fixation, euthanized adult zebrafish were opened ventrally to remove liver, spleen, intestines and reproduction organs. Kidneys remained in the body and were fixed in 4% PFA/PBS over night at 4 °C. Afterwards kidneys were prepared and embedded in paraffin (Sigma Aldrich). With a Leica RM2235 microtome, paraffin sections were cut with a thickness of 4 µm. Periodic acid Schiff reaction (Schiff's reagent by Merck, periodic acid and sodium disulfite by Roth) of the sections was done after de-paraffinization, using Tissue-Clear® (Tissue-Tek®) as xylene substitute.

Ultrafiltration assay

At 72 hpf, 5 nl of Texas-Red™ labeled 70 kDa dextran (2 ng/ml in PBS) were injected into the heart of zebrafish embryos. Embryos were kept in 96-well plates in eggwater with PTU. Images of the living embryos were taken 1, 24, and 48 h post-injection (hpi) using an inverted microscope (Leica DMI 6000 B) with a camera (Leica DFC420 C) and the Leica LAS application suite 3.8 software [29]. Decrease of maximum fluorescence intensity in the heart area was measured using NIH's ImageJ2 application [34]. The fluorescence values were compared in relative units of brightness for each fish.

Microscopic analysis and quantification

Zebrafish embryos and larvae were anesthetized with 0.003% tricaine. Phenotyping of *Tg*(*fli1:EGFP*) trunk vasculature in zebrafish larvae was carried out on an inverted microscope (Leica DMI 6000 B) with a camera (Leica DFC420 C) and the Leica LAS application suite 3.8 software at 96 hpf. In the analysis the development of new blood vessels, here referred to as 'hyperbranches', and altered blood vessels that either miss connections to others or show slight malformations were grouped as 'partially normal' and counted. Confocal imaging of *Tg*(*fli1:EGFP*) larvae and adult retinal vasculature was performed using a TCS SP5 system (Leica). Images were taken with 600 Hz, 1024 × 512 (trunk vasculature) or 1024 × 1024 pixels (retina vessels) and z-stacks were 1 µm (trunk vasculature) or 1.5 µm (retina vessels) thick. For the quantification of the retina the entire vascular area was divided into three smaller different areas according to vascular density (Fig. 3b). One quarter was characterized by low, the other quarter by high vessels density, while two quarters showed middle vessel density. Images were cut to the size of 350 × 350 µm. The lowest number of obtained squares per condition was taken as reference to adjust the number of images per condition and group to the mentioned ratio of 1(high):2(middle):1(low). Images were selected by random selection (research randomizer—http://www.randomizer.org). Within the areas new blood vessels without a lumen formed by neoangiogenesis were counted and addressed as 'hyperbranches'. Additionally, new blood vessels with a lumen, but no connection to other vessels were counted as 'protrusions', while vessels between two arcades that showed a lumen were counted as 'branches'.

For in vivo imaging of pronephric structures, embryos were embedded in 1% low melting point agarose (Promega) dissolved in E3 Medium at 48 hpf age. Images of *Tg*(*wt1b:EGFP*) embryos were taken with a Leica DFC420 C camera, attached to a Leica MZ10 F modular stereo microscope. Alterations in pronephric structures were measured and quantified by measuring the size of glomerular length, width and neck, using Leica LAS V4.8 software.

Bright field images of histological kidney slides (PAS stained) were taken, using the same microscope and software as for the phenotyping of the vasculature in zebrafish larvae. Per animal 20 Glomeruli were analyzed by a veterinary pathologist using a Leica DM 2000 microscope, checking for pathological changes, like glomerular hypertrophy, mesangial expansion, matrix deposition, glomerular hyalinosis and sclerosis, as well as cystic Bowman's spaces. Further changes as tubular atrophy and proteinaceous casts were considered. Changes were semiquantitatively categorized in four groups: 0, no significant changes; +, mild changes; ++, moderate changes; +++, significant (severe) changes.

Detection of metabolites

Detection was done in cooperation with the Metabolomics Core Technology Platform from the Centre of Organismal Studies Heidelberg. Zebrafish larvae of 96 hpf age were anesthetized with 0.003% tricaine and 40–50 were collected for the analysis. Muscle tissue of euthanized adult zebrafish was collected after overfeeding in ice cold 1% PBS with tweezers from the sides of the body, residual fluid removed and immediately frozen away. Adenosine compounds, thiols and free amino acids were extracted from the larvae with 0.3 ml of 0.1 M HCl in an ultrasonic ice-bath for 10 min. The resulting homogenates were centrifuged twice for 10 min at 4 °C and 16,400*g* to remove cell debris. Adenosines were derivatized with chloroacetaldehyde as described in Bürstenbinder et al. [35] and separated by reversed phase chromatography on an Acquity BEH C18 column (150 mm × 2.1 mm, 1.7 µm, Waters) connected to an Acquity H-class UPLC system. Prior separation, the column was heated to 42 °C and equilibrated with 5 column volumes of buffer A (5.7 mM TBAS, 30.5 mM KH_2PO_4 pH 5.8) at a flow rate of 0.45 ml/min. Separation of adenosine derivates was achieved by increasing the concentration of buffer B (2/3 acetonitrile in 1/3 buffer A) in buffer A as follows: 1 min 1% B, 1.6 min 2% B, 3 min 4.5% B, 3.7 min 11% B, 10 min 50% B, and return to 1% B in 2 min. The

separated derivates were detected by fluorescence (Acquity FLR detector, Waters, excitation 280 nm, emission 410 nm, gain 100) and quantified using ultrapure standards (Sigma). Determination of amino acid levels was done as described in Weger et al. [36].

Total glutathione was quantified by reducing disulfides with DTT followed by thiol derivatization with the fluorescent dye monobromobimane (Thiolyte, Calbiochem). For quantification of GSSG, free thiols were first blocked by NEM followed by DTT reduction and monobromobimane derivatization. GSH equivalents were calculated by subtracting GSSG from total glutathione levels. Derivatization was performed as described in Wirtz et al. [37]. UPLC-FLR analysis was carried out using the system described above. Separation was carried out using the above described UPLC-FLR system with a binary gradient of buffer A (100 mM potassium acetate, pH 5.3) and solvent B (acetonitrile) with the following gradient: 0 min 2.3% buffer B; 0.99 min 2.3%, 1 min 70%, 1.45 min 70%, and re-equilibration to 2.3% B in 1.05 min at a flow rate of 0.85 ml/min. The column (Acquity BEH Shield RP18 column, 50 mm × 2.1 mm, 1.7 µm, Waters) was maintained at 45 °C and sample temperature was kept constant at 14 °C. Monobromobimane conjugates were detected by fluorescence at 480 nm after excitation at 380 nm after separation. Data acquisition and processing was performed with the Empower3 software suite (Waters).

Fatty acids and primary metabolites were determined by semi-targeted gas chromatography-mass spectrometry (GC/MS) analysis, for which all measured values were normalized to the amount of detected ribitol in percent. For GC/MS zebrafish larvae were extracted in 180 µl of 100% MeOH for 15 min. at 70 °C with vigorous shaking. As internal standard 5 µl Ribitol (0.2 mg/ml) were added to each sample. After the addition of 100 µl chloroform samples were shaken at 37 °C for 5 min. To separate polar and organic phases, 200 µl water were added and samples were centrifuged for 10 min at 11,000 × *g*. For the derivatization, 300 µl of the polar (upper) phase were transferred to a fresh tube and dried in a speed-vac (vacuum concentrator) without heating. Pellets were re-dissolved in 20 µl methoximation reagent containing 20 mg/ml methoxyamine hydrochloride (Sigma 226904) in pyridine (Sigma 270970) and incubated for 2 h at 37 °C with shaking. For silylation, 32.2 µl *N*-methyl-*N*-(trimethylsilyl)trifluoroacetamide (MSTFA; Sigma M7891) and 2.8 µl Alkane Standard Mixture (50 mg/ml C_{10}–C_{40}; Fluka 68281) were added to each sample. After incubation for 30 min at 37 °C, samples were transferred to glass vials for GC/MS analysis. A GC/MS-QP2010 Plus (Shimadzu®) fitted with a Zebron ZB 5MS column (Phenomenex®; 30 m × 0.25 mm × 0.25 µm) was used for GC/MS analysis. The GC was operated with an injection temperature of 230 °C and 2 µl sample were injected with split mode (1:10). The GC temperature program started with a 1 min hold at 70 °C followed by a 6 °C/min ramp to 310 °C, a 20 °C/min ramp to 330 °C and a bake-out for 5 min. at 330 °C using helium as carrier gas with constant linear velocity. The MS was operated with ion source and interface temperatures of 250 °C, a solvent cut time of 6.3 min and a scan range (*m*/*z*) of 40–1000 with an event time of 0.3 s.

CN2 western blot

CN2 protein amount in *CNDP1* knockout zebrafish and wildtype controls was determined by the group of Dr. Verena Peters in Heidelberg (Dietmar-Hopp-Stoffwechselzentrum). Zebrafish embryos were collected as described in 4.2.3.8. 96 hpf old zebrafish embryos were briefly washed in PBS and homogenized in RIPA buffer (150 mmol/l NaCl, 0.5% (w/v) sodium deoxycholate, 0.1% (w/v) SDS, 50 mmol/l Tris/HCl pH 8.0, 0.1% (v/v) Triton X 100). Samples were incubated on ice for 30 min and centrifuged at 13,000*g* for 25 min. The supernatant was separated by SDS-PAGE and proteins were transferred onto a nitrocellulose membrane by semi-dry blotting with 1 mA/cm^2. The membrane was blocked over night at 4 °C with 5% milk powder (w/v) in PBS with 0.05% Tween 20 (PBS-T), following incubation at room temperature for 2 h with the primary anti-CN2 antibody (1:2000; Rabbit polyclonal, 14925-1-AP, proteintech) in PBS-T with 5% milk powder. After washing, the blot was incubated with a secondary horseradish peroxidase-conjugated antibody (1:20,000; A0545, Sigma-Aldrich) in PBS-T for 1 h at room temperature. β-Actin antibody (1:2500; A2228, Sigma-Aldrich) was used as internal control. Proteins were visualized with ECL detection reagent (Biorad) and a western blot detection system (Peqlab). In silico densitometry was performed with ImageJ v1.15d (public domain).

Determination of methylglyoxal (MG)

The determination of MG by stable isotopic dilution analysis via LC–MS/MS was described previously [38]. Briefly, frozen zebrafish embryos (approx. 50) were treated with precipitation solution (Trichloracetic acid 20% w/v in 0.9% NaCl), incubated with an "heavy" internal standard and derivatized with 1,2-diaminobenzene. Quantification was carried out using a XEVO TQ-S tandem quadrupole mass spectrometer (Waters®).

Incubation with MG

About 60 eggs were incubated at 28.5 °C in a 10 cm Petri dish with 30 ml solution that was changed daily. The solution contained egg water, 500 µM MG and 0.003% PTU.

Determination of glucose

Embryos were lysed in sodium phosphate buffer (100 mM; pH 7.4 + 0.1% Triton X) by sonication (Biodisruptor™) 30 s. on/off for a total of 20 cycles. Samples were then centrifuged (5 min; 4 °C; 14,000 rpm) and supernatants were collected. Supernatant was deproteinized with the deproteinizing sample preparation kit (Biovision) according to the manufactures protocol. Glucose measurement was performed with the Amplex™ Red Glucose/Glucose Oxidase Assay Kit (Invitrogen) following the manufacturer's protocol.

Overfeeding of adult zebrafish

Adult male zebrafish were set in groups according to genotype and feeding. The feeding procedure was adapted from Oka 2010 [39]. For normal feeding: each fish received one time a normal amount of artemia (5 mg dry weight artemia cysts/day) in the morning and one-time dry food in the afternoon. For overfeeding: fish were overfed by receiving three times artemia (3 × 20 mg dry weight artemia cysts/day) with 2 h break between the feedings and one-time dry food in the afternoon. This protocol was followed over 8 weeks. Afterwards animals were killed for experiments.

Computer programs and statistics

Determination of fluorescence intensity in the ultrafiltration assay was done using ImageJ2 application [34]. Analysis of retinal vasculature was carried out using LAS AF Lite Software from Leica for taking screen shots, Gimp2 for image cutting and ImageJ2 for quantification (see Wiggenhauser et al. [33]). For GC/MS analysis the "GCMS solution" software (Shimadzu®) was used for data processing. Results are expressed as mean with standard deviation (mean ± SD). Statistical significance between different groups was analyzed using Student's *t* test, Mann–Whitney *U* test, one-way ANOVA (either followed by Bonferroni's Tukey's or Sidak's multiple comparison) or Kruskal–Wallis test (followed by Dunn's multiple comparison) in GraphPad Prism 6.01. *p* values of ≤ 0.05 were considered as significant: $^{*}p \leq 0.05$, $^{**}p \leq 0.01$, $^{***}p \leq 0.001$.

Results

Organ specific differences of the carnosinase system in zebrafish

Besides the discovery of carnosine-like peptides in the nervous system of zebrafish embryos [22], the presence of its degrading enzyme CN1 has not been described before. Therefore, we aimed to analyze if CN1 activity is present in zebrafish. Previous studies could already show differences between human and rodents, e.g., CN1 expression is specific in human brain tissue and kidney, whereas in mice and rats it is solely found in the kidney [7, 31]. In a first step we performed an amino acid sequence alignment to compare CN1 proteins of zebrafish, mouse and human. The alignment indicated high similarities between the species for the active catalytic domain, metal binding sites and peptidase dimerization domain. A signal peptide sequence was also identified in zebrafish CN1 which is similar to human CN1, but is not present in mouse CN1 (Fig. 1a). To investigate potential differences of CN1 activity in various tissues, we isolated brain and kidney tissue of adult zebrafish of both sexes. It was identified that CN1 activity is present in the kidney and brain of adult zebrafish, where the brain exhibits a significantly higher CN1 activity (Fig. 1b); yet, the sex has no influence on CN1 activity. Carnosine as one of the substrates of CN1 was detected in brain and kidney of adult zebrafish (Fig. 1c). The concentrations of anserine as another substrate for CN1, were higher in the kidney than in the brain of female fish (Fig. 1d). Taken together, the data identified CN1, carnosine and anserine in zebrafish organs, with higher dipeptide contents in the kidney.

Generation and validation of CNDP1$^{-/-}$ zebrafish

Since *CNDP1* knock out animal models do not exist thus far and to analyze the function of CN1 in zebrafish development, we used the CRISPR-Cas9 technology to generate knockout animals. Therefore, we used a gRNA to specifically target the gene that resembles *CNDP1* in zebrafish (Gene ID ENSDARG00000069583). Following the injection of the gRNA together with Cas9 mRNA, we identified three different frame-shift mutations in knockout animals and all mutations lead to the formation of a Stop-codon (Fig. 2a). *CNDP1*$^{-/-}$ knockout embryos are viable and developed without obvious alterations (Fig. 2b). To assess if the respective mutations cause the translation of a non-functional CN1 protein, we measured the CN1 activity by detecting the degradation of carnosine along with the concentrations of carnosine and anserine in mutant animals. In *CNDP1*$^{-/-}$ animals, degradation of carnosine was strongly reduced (Fig. 3a), with significantly increased carnosine concentrations, whereas anserine concentrations remained unaltered (Fig. 3b). Thus, the data have proven a successful generation of *CNDP1* knockout zebrafish.

Normal vascular development and maturation in CNDP1$^{-/-}$ zebrafish

The early development of the vascular system is essential for zebrafish to ensure a normal development of the

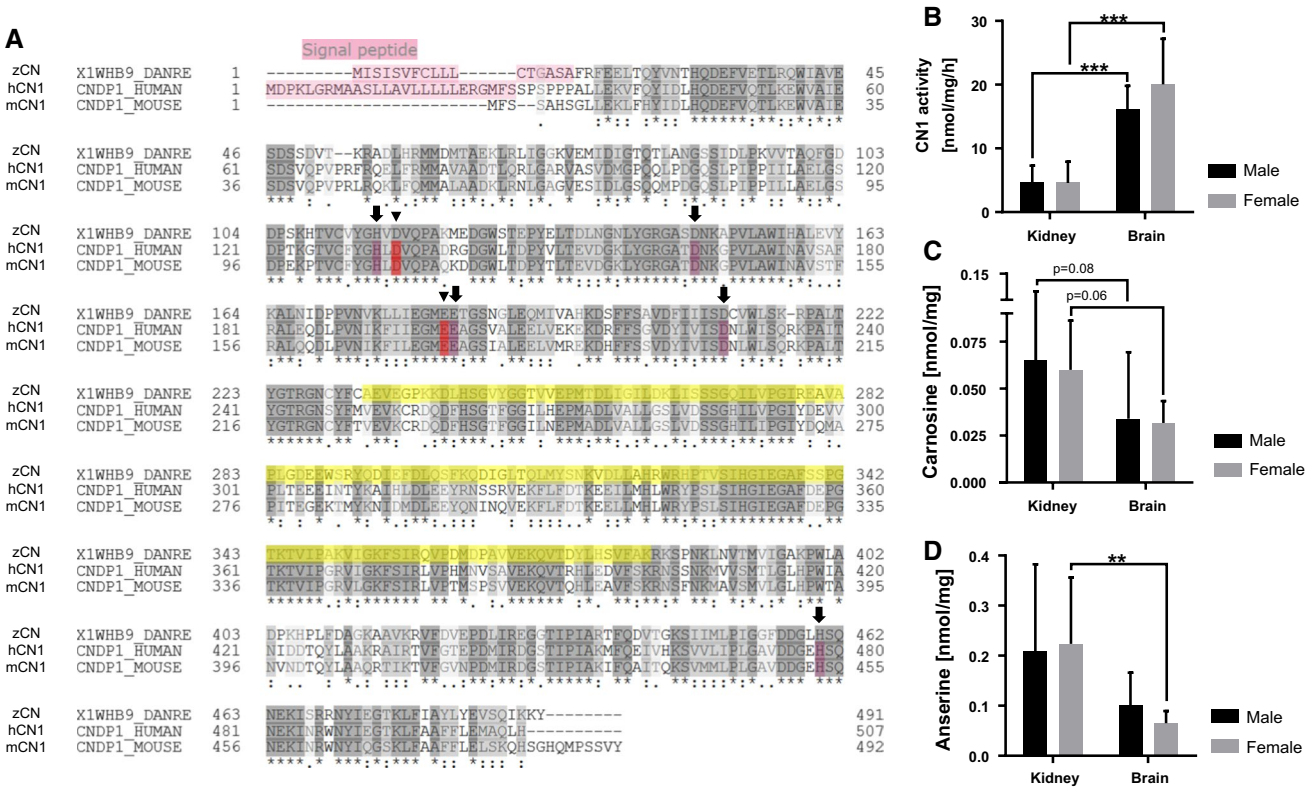

Fig. 1 Sequence alignment of carnosinases across different species and detection of CN1 activity and its substrates in adult zebrafish organs. **a** Amino acid alignment showed a high similarity between the different species of the active (arrow head), metal binding sites (arrow) and of peptidase dimerization domain (yellow); *zCN* zebrafish carnosine dipeptidase, *hCN1* human carnosinase1, *mCN1* mouse carnosinase1. **b** CN1 activity in adult zebrafish was higher in brain than in kidney tissue. CN1 activity was determined by measuring the degradation of carnosine; **c** carnosine and **d** anserine concentrations were higher in kidney than brain tissue with similar concentrations in males and females. Carnosine and anserine concentrations were measured by HPLC, data were analyzed using Student's *t* test, $*p \leq 0.05$, **b** males $n=7$, females $n=6$–7, **c** males $n=10$, females $n=6$–8, **d** $n=8$ per group, mean ± SD

entire organism. Likewise, alterations of the vasculature are often causes of organ damage in several disease conditions [40]. To address the question if the loss of *CNDP1* impairs vascular development, we generated animals with a *Tg*(*fli1:EGFP*) background. In these animals, EGFP is expressed under the control of the *fli1* promotor and thus labels the entire vasculature through the whole lifetime [27]. Subsequently, the vascular system in *CNDP1*$^{-/-}$ animals was analyzed in early development and in adult organs. At 96 hpf *CNDP1*$^{-/-}$ zebrafish larvae showed a normal vasculature consisting of the dorsal aorta, posterior cardinal vein, intersegmental vessels, and parachordal lymphangioblast. In the quantification of the vascular architecture no significant differences between wildtype and knockout larvae were visible (Fig. 4). To analyze the mature vasculature in adult *CNDP1* knockout animals, we dissected the retinal vasculature according to a recently published protocol [33]; yet, vascular structures in the retina of adult animals remained unaffected (Fig. 5), indicating that the knockout of *CNDP1* has no impairing effect on vascular development and maturation in zebrafish.

CNDP1 knockout causes minor alterations in zebrafish kidney development which does not persist in adulthood

The published data on the function of carnosine and kidney function under diabetic conditions have suggested a protective function for carnosine in these pathologies, since external administration of carnosine to mice improved glucose homeostasis and improved symptoms of DN in diabetic animals [16, 18, 19, 39]. Yet, is has not been studied before if an increase of carnosine could interfere with kidney development by itself. Thus, we took advantage of the *CNDP1*$^{-/-}$ zebrafish which show enhanced carnosine concentrations (Fig. 3). For the morphological analysis of the embryonic kidney (pronephros), *CNDP1*$^{-/-}$ animals with *Tg*(*wt1b:EGFP*) background were generated. Those animals show a pronephros-specific GFP-expression, labeling the glomerulus, the neck and the tubular structures that together form the pronephros [26]. In 48-hpf-old *CNDP1*$^{-/-}$ zebrafish embryos the glomerular length was reduced (Fig. 6a); though, the function of the pronephros

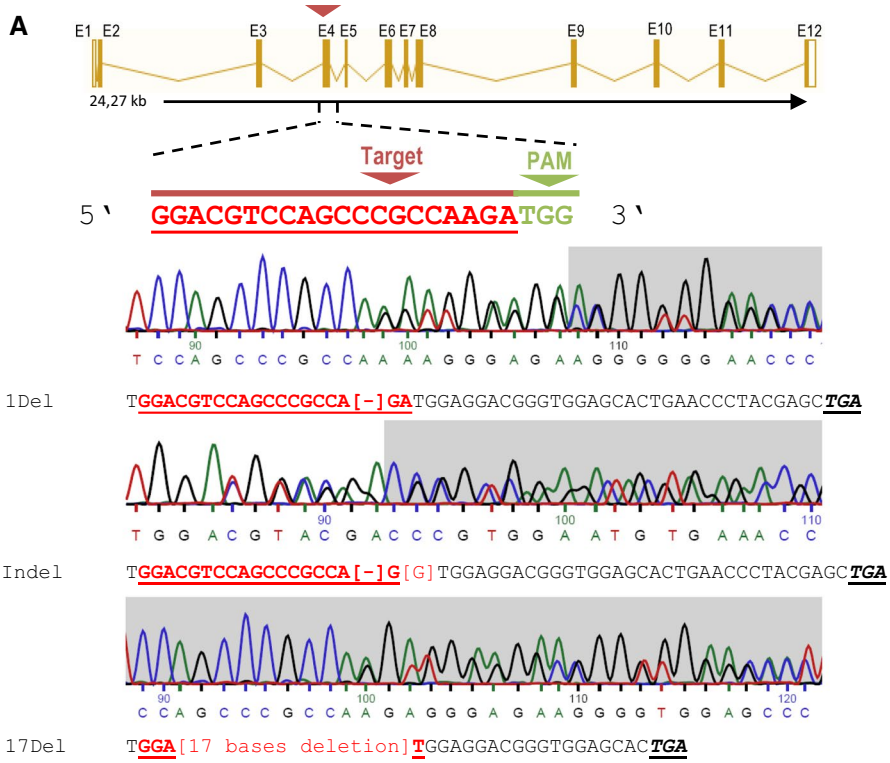

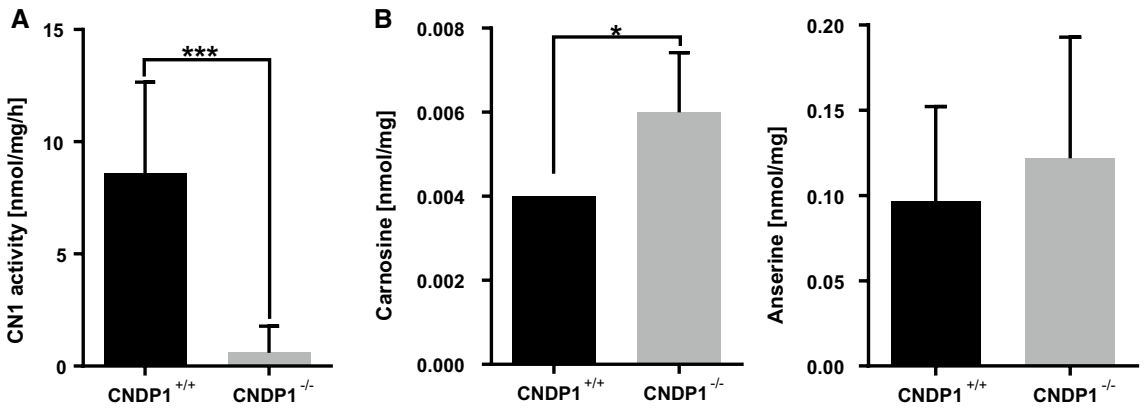

Fig. 2 Generation of *CNDP1* knockout animals. **a** Binding site of the Cndp1-CRISPR gRNA in exon 4 [exon–intron illustration modified from the Ensembl database]. Three different mutations were identified, all leading to frameshift mutations and showing no CN1 activity. Heterozygous mutations are shown as sequencing chromatogram. Angular brackets indicate deletions or indels, Stop codons are in black, italic and underlined; *PAM* protospacer adjacent motif. **b** *CNDP1*$^{-/-}$ zebrafish showed a normal development in both transgenic backgrounds (*Tg*(*fli1:eGFP*) and *Tg*(*wt1b:EGFP*)). Bright field image of 96 hpf old larvae, black scale bar is 1 mm

Fig. 3 Validation of *CNDP1* knockout animals. **a** CN1 activity was strongly reduced in brain tissue of adult *CNDP1* knockout animals. CN1 activity was determined by measuring carnosine degradation. **b** Carnosine was increased in the brain tissue of adult *CNDP1*$^{-/-}$ homozygous, while anserine levels were not altered; Carnosine and anserine concentrations were measured by HPLC; Data were analyzed using Student's *t* test, $*p \leq 0.05$, $***p \leq 0.001$, **a** $n = 8$, **b** carnosine $n = 4$, anserin $n = 6$, mean ± SD

remained unaffected (Fig. 6b). Based on this finding we addressed the question if the pronephros developmental impairments in *CNDP1*$^{-/-}$ zebrafish embryos persist in adult animals and we therefore performed a histological analysis of adult *CNDP1*$^{-/-}$ kidneys. PAS stained paraffin sections could not show obvious differences in *CNDP1*$^{-/-}$ mutants focusing on glomerular and tubular structures as compared to wildtype kidneys (Fig. 6c–h and Supporting information

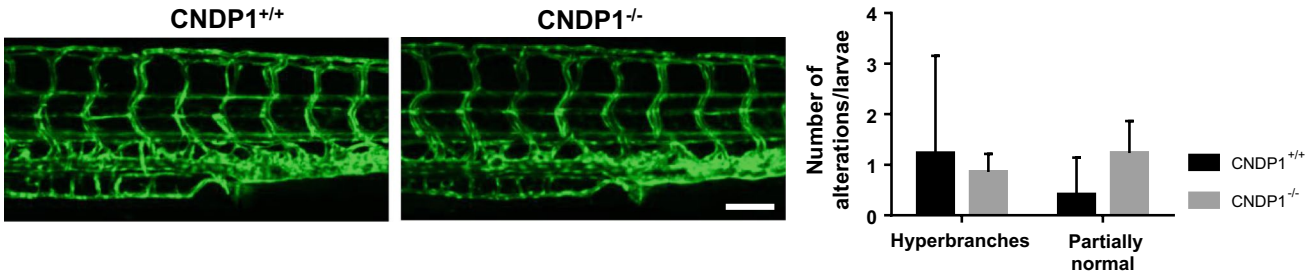

Fig. 4 Vascular structures are unaltered in *CNDP1*$^{-/-}$ zebrafish larvae. *CNDP1*$^{-/-}$ larvae showed no alterations in their trunk vasculature compared to *CNDP1*$^{+/+}$ animals at 96 hpf. The trunk vasculature was analyzed in *Tg*(*fli1:eGFP*) embryos by fluorescence and confocal microscopy; white scale bar is 100 µm; data were analyzed using Mann–Whitney *U* test, CNDP1$^{+/+}$ $n=22$, CNDP1$^{-/-}$ $n=14$, mean ± SD

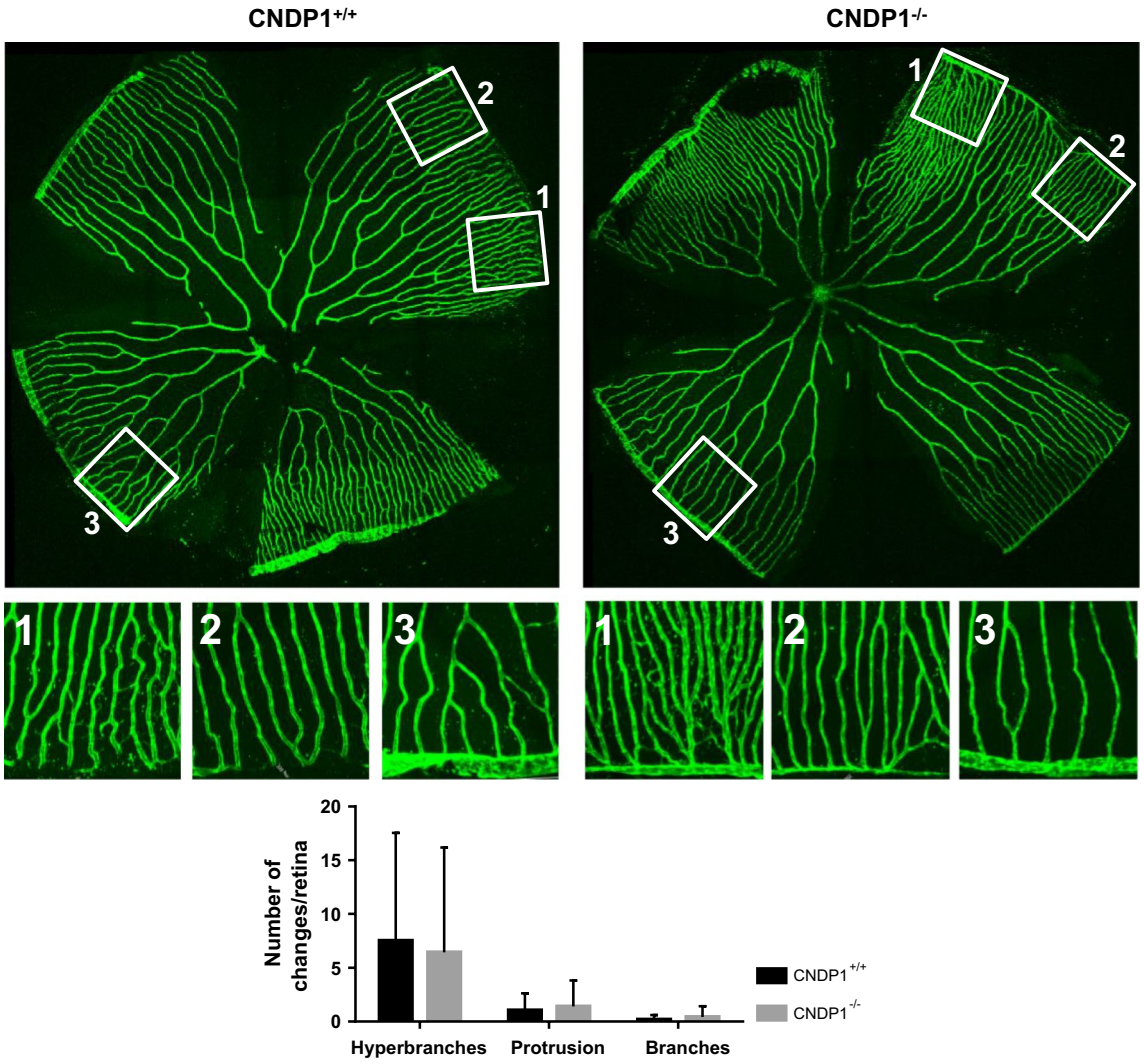

Fig. 5 Retinal vasculature is unaltered in adult *CNDP1*$^{-/-}$ zebrafish. *CNDP1*$^{-/-}$ animals showed a normal architecture of retinal vessels compared to wildtype animals. Retinal vasculature was isolated from adult *CNDP1*$^{-/-}$ *Tg*(*fli1:eGFP*) animals and analyzed by confocal microscopy; for quantification the vascular network was divided in three different groups according to their naturally occurring vessel density (according to Wiggenhauser et al. [33]). Every group is exemplarily shown: *1* hyperdense area, *2* middle dense area, *3* low dense area; Each square is 350×350 µm; data were analyzed using Mann–Whitney *U* test, $n=4$ animals per group (CNDP1$^{+/+}$ $n=64$ petals, CNDP1$^{-/-}$ $n=32$), mean ± SD

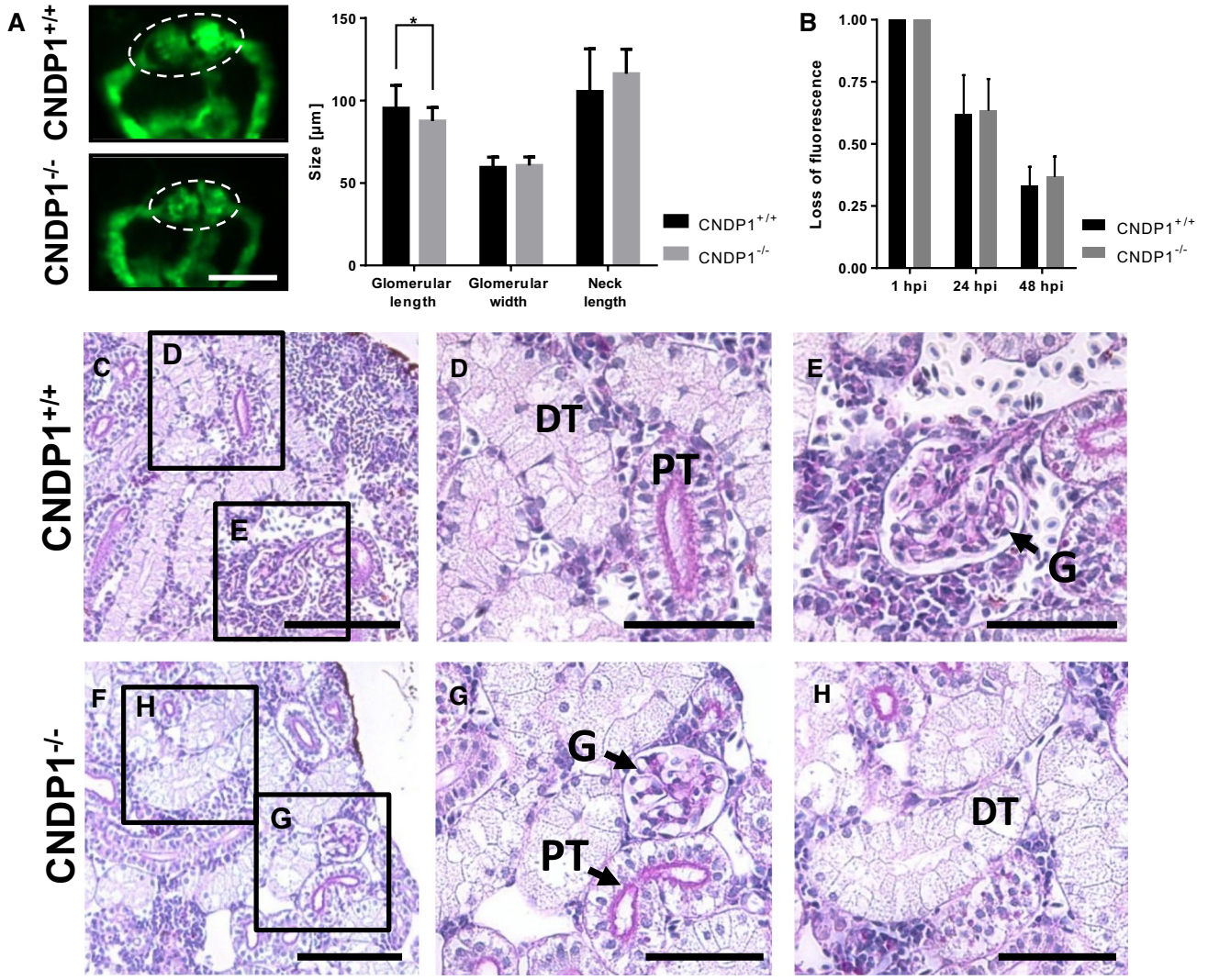

Fig. 6 *CNDP1* knockout embryos show minor pronephros alterations, but adult kidney morphology is normal. **a** Glomerular length was decreased in *CNDP1*$^{-/-}$ *Tg*(*wt1b:EGFP*) embryos at 48 hpf. Glomerulus is indicated by dotted lines, white scale bar is 100 µm, CNDP1$^{+/+}$ $n=29$, CNDP1$^{-/-}$ $n=32$ embryos; **b** *CNDP1*$^{-/-}$ larvae showed no differences in the loss of fluorescence intensity after intracardial injection of 70 kDa labeled dextran. CNDP1$^{+/+}$ $n=24$, CNDP1$^{-/-}$ $n=40$; **f**–**h** renal structures of adult *CNDP1*$^{-/-}$ did not show obvious alterations in kidney morphology compared to wildtype (**c**–**e**) animals. Paraffin sections (4 µm) were analyzed with light microscopy after PAS-staining; $n=4$ animal each; *DT* distal tubule, *G* glomerulus, *PT* proximal tubule, **c**, **f** scale bar is 100 µm; **d**, **e**, **g**, **h** scale bar is 50 µm; data were analyzed using Student's *t* test, $^{*}p \leq 0.05$, mean ± SD

Fig. S1). Thus, the knockout of *CNDP1* in zebrafish results in a transient developmental phenotype of the pronephros, but normalizes during further ontogenesis.

Altered amino acid metabolism in CNDP1 knockout zebrafish is not compensated by CN2

Considering the phenotypical normal appearance of *CNDP1*$^{-/-}$ larvae and adults, we aimed to perform a biochemical analysis of *CNDP1*$^{-/-}$ animals to identify potential pathways where CN1 could be involved, apart from its known function to cleave carnosine in zebrafish (Fig. 1). Thus, we analyzed 96 hpf old zebrafish larvae via a metabolomic screening, targeting amino acids, thiols, adenosines, fatty acids and a set of primary metabolites. Hereby we could show that no other pathways, except for the amino acid metabolism, were affected by *CNDP1* knockout (Supporting information Figure S2–S6). Specifically, five amino acids, namely glycine, cysteine, histidine, alanine, and serine were significantly decreased in mutant animals (Fig. 7a, b). A metabolic connection between serine, glycine and cysteine synthesis has been well documented, showing that glycine and serine can be precursors of each other, while cysteine is generated from serine over

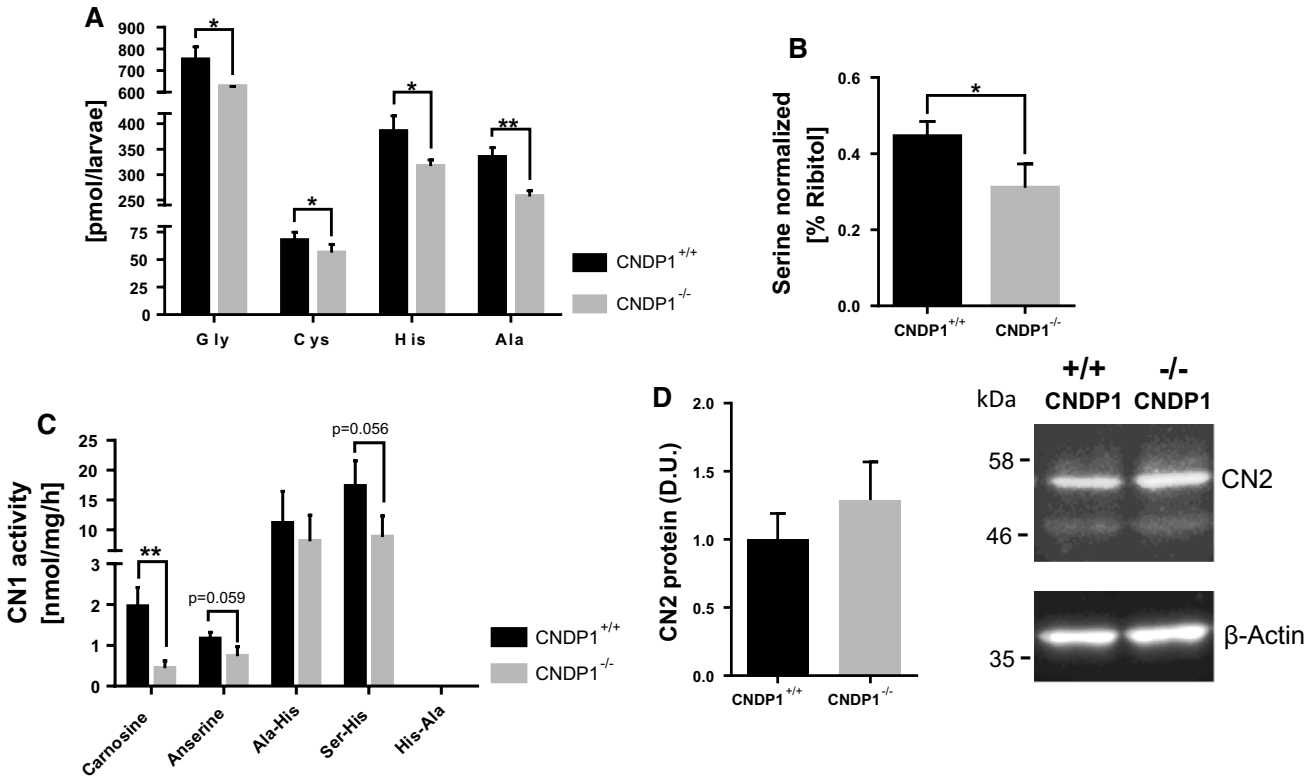

Fig. 7 *CNDP1* knockout larvae show an altered amino acid profile and decreased activity for Ser–His degradation. Amino acids were measured in 96 hpf old larvae by **a** UPLC-MS and **b** semi-targeted GC-MS-analysis and showed a significant decrease of **a** glycine, cysteine, histidine and alanine as well as **b** serine. **c** *CNDP1* knockout caused a decrease in the activity to degrade Ser–His. Activity for His-Ala = 0.00 nmol/mg/h. Activities were determined by the quantification of histidine release in lysates of 96 hpf old larvae. **d** Western blot against CN2 showed no upregulation of CN2 protein in lysates of 96 hpf old *CNDP1*$^{-/-}$ larvae probed with anti-CNDP2 and anti-β-actin antibody as a loading control. Relative emission of antibody-labeled CN2 protein was determined in densitometric units (D.U.). $n = 3$. Data were analyzed using Student's t test, $^{*}p \leq 0.05$, $^{**}p \leq 0.01$; Cys $n = 6$, Gly, His, Ala, Ser $n = 3$ each, **c** $n = 3$, mean ± SD

the methionine-*S*-adenosylmethionine cycle [41] and the coupled transsulfuration pathway [42]. More importantly, the decrease of histidine and alanine is most likely linked to the increased concentrations of carnosine in the *CNDP1* mutants, which suggests that these amino acids are stored as carnosine and hereby less abundantly available. Thus, the data show a novel function for CN1 in the formation of serine, glycine and cysteine, which needs now to be studied in different disease conditions. To support this evidence, we determined if CN1 can degrade other histidine-containing dipeptides, like Ala–His, Ser–His and His–Ala. We could show that CN1 is able to degrade Ala–His and Ser–His, but not His–Ala, where no activity for it could be determined at all (activity for His-Ala = 0.00 nmol/mg/h ± 0.00). In *CNDP1*$^{-/-}$ mutants, we observed a trend for less Ser–His degradation (Fig. 7c), which implies that zebrafish CN1 can degrade other dipeptides as well but remains more specific for the degradation of carnosine. With a western blot against CN2 protein we could show that CN2 is not upregulated in a compensatory manner by the loss of *CNDP1* (Fig. 7d).

A CNDP1 knockout is not beneficial to prevent diabetes-induced organ complications in zebrafish, but protects from profound weight gain

Under normal physiological conditions CN1 hydrolyzes carnosine depending from its metabolic demands [7, 31, 43]. Nevertheless, under pathophysiological conditions CN1 activity can increase dramatically. One prime example is the reactive metabolite methylglyoxal (MG), which is increasingly formed under diabetic conditions, induces post-translational modifications and thereby alters the function of the affected proteins. Increased concentrations of MG are also known to form advanced glycation end products [44, 45]. In vitro and in vivo experiments using cultured kidney cells overexpressing human *CNDP1* or by analyzing kidneys from diabetic mice, demonstrated that MG increases CN1 activity by direct carbonylation, which resulted in a decreased availability of carnosine [20].

Based on these findings we incubated zebrafish larvae over time in MG containing medium [46] to ascertain if MG alters CN1 activity in zebrafish as well. A significant

increase of CN1 activity at 96 hpf for larvae incubated in MG was found (Fig. 8a), but this was only accompanied by a minor decrease of carnosine (Fig. 8b). Thus, MG can also alter CN1 activity in zebrafish. In a previous study we showed that MG causes organ malformations in zebrafish larvae, resulting in neovascularization of the trunk vasculature [46]. Based on the findings we incubated *Tg(fli1:EGFP) CNDP1* mutant embryos in MG containing medium, determined internal MG concentrations at 48 hpf and analyzed vascular structures at 96 hpf. MG levels were significantly increased in zebrafish, but remained unchanged in *CNDP1*$^{-/-}$ embryos (Fig. 9a). Analysis of the treated embryos, however, did not identify beneficial effects of *CNDP1* knockout on MG induced pathological vessel sprouting (Fig. 9b). These results are contrary to the increased carnosine concentrations in knockout animals that would imply a protective scavenging of MG. Hence, the data also suggest that the internal increase of carnosine in *CNDP1*$^{-/-}$ animals may not be sufficient to quench MG.

Furthermore, we also tested glucose itself as an inducer of organ damage under diabetic conditions. A recent publication showed that the zebrafish pronephros is sensitive to increased glucose concentrations resulting in morphological malformations [29], with similar cellular kidney alterations seen in patients suffering from DN. In these experimental settings, the knockdown of the transcription factor *pdx1* causes glucose to increase [30, 46, 47]. The beneficial

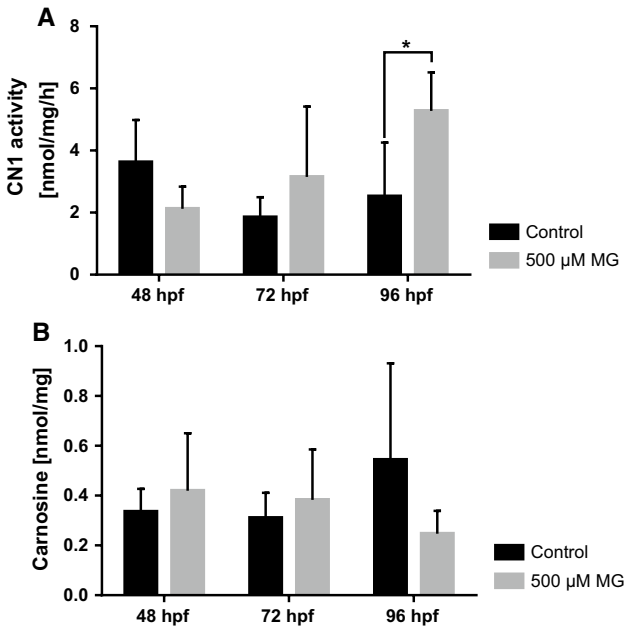

Fig. 8 MG increases CN1 activity in zebrafish. Detection of CN1 activity (**a**) and carnosine (**b**) in zebrafish larvae. Incubation of embryos with 500 µM MG increased CN1 activity at 96 hpf (**a**) which caused a decrease of carnosine; data were analyzed using Student's *t* test, $*p \leq 0.05$, **a** $n=4$, **b** $n=3$, mean ± SD

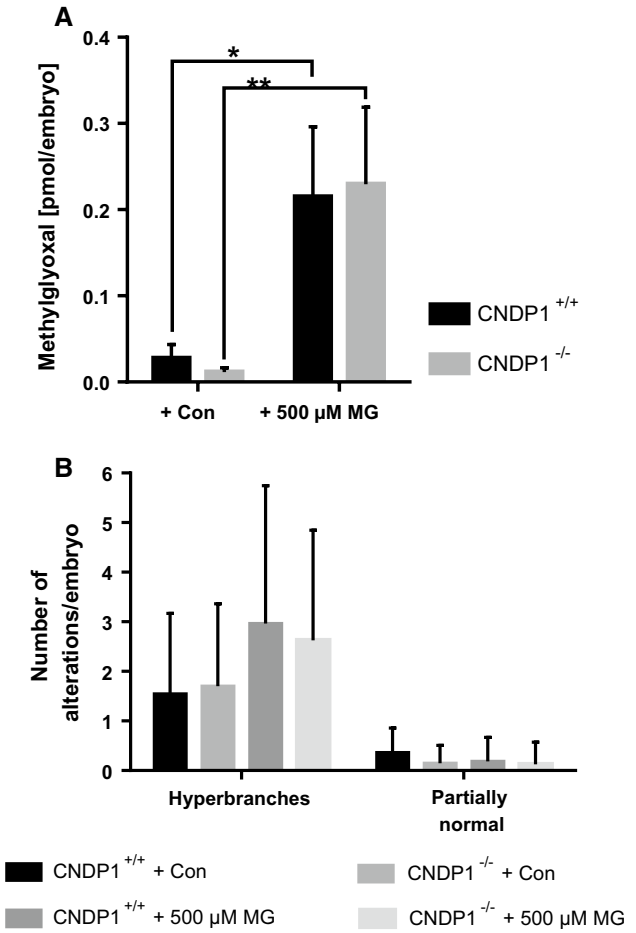

Fig. 9 *CNDP1* knockout does not protect from internal increases of MG or rescues MG-induced vascular alterations. **a** Loss of CNDP1 did not protect from an increase of internal MG concentrations by MG incubation. MG was measured in lysates of 48-hpf-old embryos by LC–MS/MS; data were analyzed using one-way ANOVA with Bonferroni's multiple comparison, $n=3$, $*p \leq 0.05$, mean ± SD; **b** incubation of *Tg(fli1:eGFP)* zebrafish larvae with 500 µM MG lead to an increase of hyperbranches at 96 hpf, which could not be restored upon *CNDP1* knockout. Embryos were analyzed via fluorescence microscopy; data were analyzed using Kruskal–Wallis test followed by Dunn's multiple comparison; *Con* control incubation, CNDP1$^{+/+}$ + Con $n=22$, CNDP1$^{-/-}$ + Con $n=27$, CNDP1$^{+/+}$ + 500 µm MG $n=27$, CNDP1$^{-/-}$ + 500 µm MG $n=24$, mean ± SD

effects of carnosine for patients with diabetic kidney diseases are a highly relevant topic. A recent publication has suggested that carnosine supplementation in diabetic mice leads to the restoration of the glomerular filtration barrier, improved glucose metabolism and albuminuria [18]. Based on these findings and our own data of increased carnosine in zebrafish in *CNDP1*$^{-/-}$ animals (Fig. 2), we aimed to determine if the internal increase in carnosine in *CNDP1*$^{-/-}$ animals has renoprotective effects in a nephropathy like setting. Therefore, we induced hyperglycemia in *CNDP1* knockout embryos and analyzed the pronephros at 48 hpf as well as internal glucose levels. As previously

shown *pdx1* knockdown induces hyperglycemia and resulted in an increase in the glomerular length with a shortened neck structure. However, hyperglycemic animals did not show an improvement of pronephric structures upon *CNDP1* knockout (Fig. 10c). Glucose measurements in these animals supported these results, showing that a *CNDP1* knock out does not improve hyperglycemia (Fig. 10a). Similar findings could be observed for the vasculature in Tg(fli1:EGFP) larvae at 96 hpf where *pdx1* knock down-induced vessel alterations could not be rescued in CNDP1$^{-/-}$ animals (Fig. 10b).

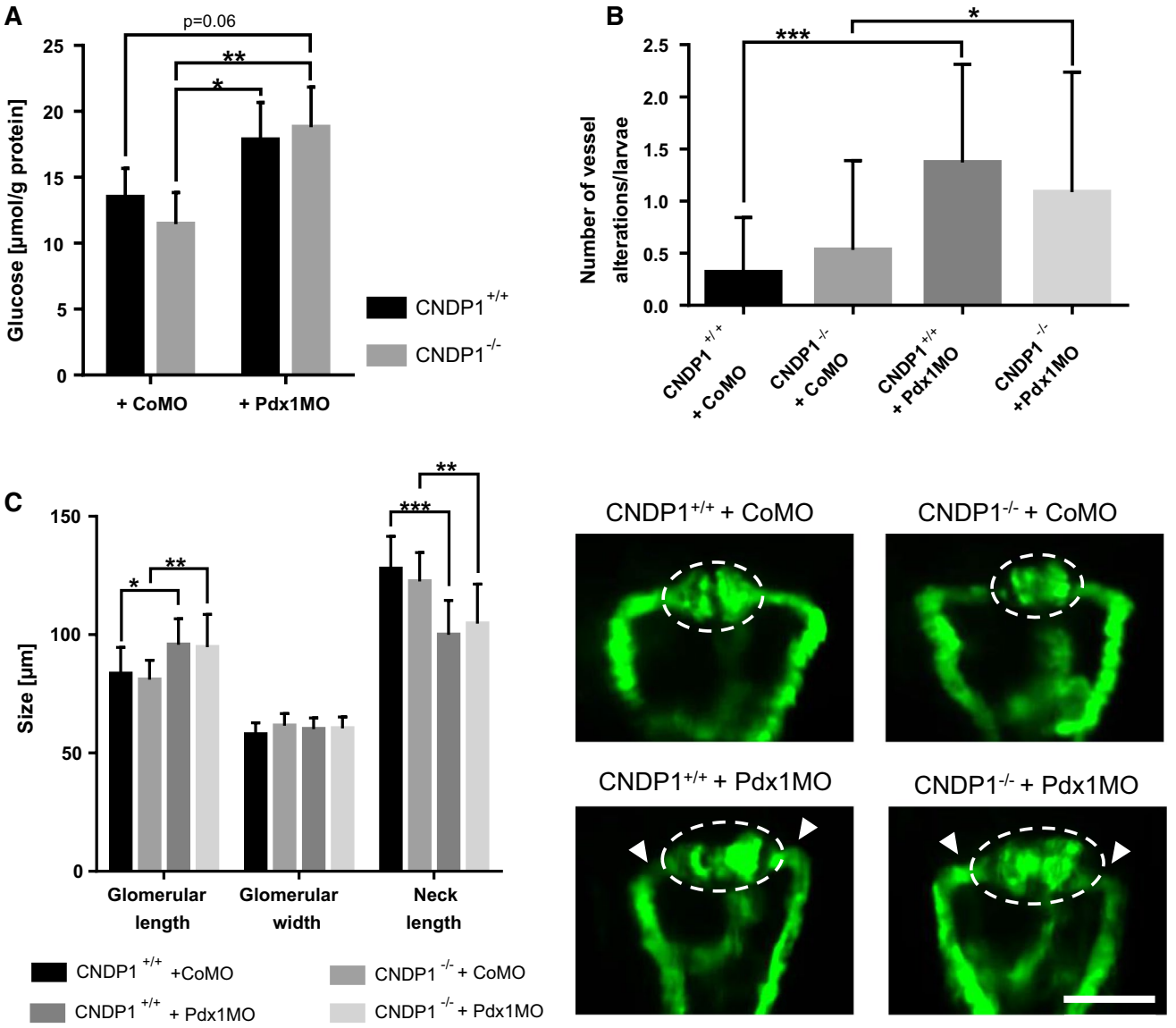

Fig. 10 *CNDP1* knockout can not rescue hyperglycemia-induced vascular or pronephric alterations and does not lower increased glucose concentrations in zebrafish embryos. Hyperglycemia was induced by *pdx1* morpholino (Pdx1MO) injection in *CNDP1*$^{+/+}$ and *CNDP1*$^{-/-}$ eggs. **a** *CNDP1* knockout did not protect from elevated glucose levels during hyperglycemia. Glucose was measured in lysates of deproteinized 48-hpf-old embryos by detecting the change of fluorescence during the reaction of glucose oxidase with D-glucose; $n=4$; data were analyzed using one-way ANOVA with Tukey's multiple comparison; **b** Hyperglycemia increased the number of vessel alterations in *Tg*(*fli1:eGFP*) 96-hpf-old zebrafish larvae, which was not restored by *CNDP1* knockout. Embryos were analyzed via fluorescence microscopy; CNDP1$^{+/+}$ + CoMO $n=38$, CNDP1$^{-/-}$ + CoMO $n=47$, CNDP1$^{+/+}$ + Pdx1MO $n=35$, CNDP1$^{-/-}$ + Pdx1MO $n=46$, data were analyzed using Kruskal–Wallis test followed by Dunn's multiple comparison; **c** hyperglycemia-induced alterations of the pronephros were not restored in *CNDP1*$^{-/-}$ embryos. Pronephric structures were quantified in *Tg*(*wt1b:EGFP*) embryos at 48 hpf via fluorescence microscopy. Glomerular structures are indicated by the dotted line. Arrowheads show the shortened neck; *CoMO* control morpholino injected, white scale bar is 100 µm; CNDP1$^{+/+}$ + CoMO $n=13$, CNDP1$^{-/-}$ + CoMO $n=15$, CNDP1$^{+/+}$ + Pdx1MO $n=18$, CNDP1$^{-/-}$ + Pdx1MO $n=19$, data were analyzed using one-way ANOVA with Sidak's multiple comparison. *$p\leq0.05$, **$p\leq0.01$, ***$p\leq0.001$, mean ± SD

Beneficial effects of carnosine and it's administration during metabolic syndrome is a highly discussed form of therapy [48, 49]. To assess this, we overfed *CNDP1*$^{-/-}$ and wildtype animals for 8 weeks and killed them afterwards to examine body weight gain. Overfeeding resulted in a significant weight gain in both genotypes when compared to weights at the beginning. However, when compared to normal fed animals only overfed wildtype animals showed a significant increase in body weight, while overfed *CNDP1* knockout animals did not gain more weight. Yet, fasting blood glucose levels remained unaltered in both groups (Fig. 11a, b). Likewise, an extended metabolome analysis in muscles of CNDP1$^{-/-}$ animals for metabolites, including several fatty acids and primary metabolites, which may explain body weight differences in the overfeeding groups, did not show any changes (Supporting information Figure S7 and S8). This suggests a protective effect of *CNDP1* knockout on body weight gain. But further investigations for actions like restraining weight gain in people with poor metabolic control would be necessary.

Taken together, diabetes induced organ alterations in zebrafish by inducing hyperglycemia or increasing MG, could not be rescued in *CNDP1*$^{-/-}$ animals. This suggests that the knockout of *CNDP1* does not lead to therapeutically relevant concentrations of carnosine that can prevent vascular or renal organ alterations under diabetic conditions.

Discussion

In this study, we have analyzed for the first time the developmental and pathological function of the carnosine−carnosinase system in zebrafish. We have generated and characterized a zebrafish knockout model for *CNDP1*, showing that: (1) carnosine, anserine and CN1 activity are present in zebrafish, with the ability to degrade other dipeptides besides carnosine, (2) *CNDP1*$^{-/-}$ animals are viable and develop normally, but show an altered amino acid profile and (3) the knockout of *CNDP1* can increase carnosine concentrations in vivo, protects to some degree from increased weight gain, but is insufficient to prevent diabetes induced complications.

The protein sequence alignment of human and zebrafish CN1 displayed a signal peptide sequence, which is not found in mice. This suggests that zebrafish CN1 acts as a secreted protein similar to human CN1, that is secreted from the liver into the blood serum [7], and emphasizes *CNDP1*$^{-/-}$ zebrafish as a novel animal model to study physiological and pathological functions of human CN1. The analysis of CN1 in zebrafish showed that CN1 activity is already present in embryos and can degrade carnosine as in humans. In adult zebrafish, CN1 activity increases and this finding again correlates with its human counterpart [6, 50]. Even though sex specific differences in zebrafish CN1 activity, as in humans [51], could not be found in zebrafish. As specific substrates for zebrafish CN1, we identified carnosine-like peptides as well as anserine. The concentrations of anserine were even higher than those of carnosine, which was also reported in mice [52] and for the human kidney

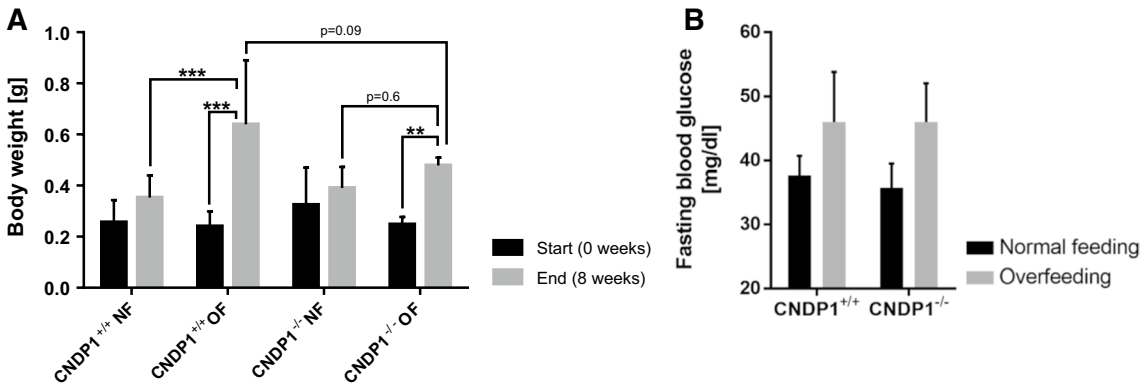

Fig. 11 CNDP1 knockout animals gain less weight upon overfeeding but do not show altered blood glucose levels. **a** Overfeeding of 8 weeks resulted in increased body weight. But overfed CNDP1$^{-/-}$ animals gained not more weight than normal fed CNDP1$^{-/-}$ animals in comparison to wildtype individuals. The animals were weighted before and after 8 weeks. *NF* normal feeding, *OF* overfeeding, CNDP1$^{+/+}$ NF $n=7$, CNDP1$^{+/+}$ OF $n=6$, CNDP1$^{-/-}$ NF $n=8$, CNDP1$^{-/-}$ OF $n=7$, $^{**}p \leq 0.01$, $^{***}p \leq 0.001$; **b** fasting blood glucose levels were not altered between *CNDP1* wildtype and mutant zebrafish after 8 weeks of normal and overfeeding. Blood was collected after one night of fasting from the caudal vein with a glass needle and glucose was measured with a glucometer. CNDP1$^{+/+}$ normal feeding $n=3$, CNDP1$^{+/+}$ overfeeding $n=3$, CNDP1$^{-/-}$ normal feeding $n=4$, CNDP1$^{-/-}$ overfeeding $n=3$. Data were analyzed using one-way ANOVA with Sidak's multiple comparison, mean ± SD

[31]. Anserine is also a protective factor by acting as an antioxidant against detrimental effects of oxygen radicals and toxic lipid-derived reactive carbonyl species [31, 48, 53]. Recently it was shown that anserine treatment in diabetic mice also improved glucose homeostasis and nephropathy [54]. Using the CRISPR-Cas9 technology, we generated the first zebrafish *CNDP1* mutant and validated it by showing loss of CN1 activity in the different mutants. Furthermore, the knockout of *CNDP1* resulted in increased carnosine levels, supporting the efficiency of our knockout strategy. Besides CN1's function being a dipeptidase for carnosine and anserine, it was unknown how CN1 is involved in the global amino acid metabolism and whether CN1 also regulates other biochemical and metabolic pathways. Thus, we performed a global metabolomic analysis for several different metabolites and found that the depletion of CN1 does not affect the thiol or adenosine metabolism, as well as fatty acid composition or a variety of primary metabolites as part of other metabolic pathways. However, very distinct alterations in some amino acids were observed, indicating that carnosinase 1 in zebrafish is not only specific for carnosine, but also for other histidine-containing dipeptides. Carnosine and anserine concentrations are about five- to tenfold lower in zebrafish compared to mice, and it was discussed whether also free histidine contribute to the function of histidine-containing dipeptides in fish [5]. Whereas cellular carnosine levels are elevated in the knockout, anserine levels remained unaltered, suggesting that anserine is not a preferred substrate for zebrafish CN1 in contrast to rodent CN1. The decrease of alanine and histidine could imply that both amino acids are stored as dipeptides which would be new substrates for CN1 in zebrafish. Although this requires further investigations, the data suggest that on demand CN1 rapidly increases alanine and histidine in cells and therefore act as a gatekeeper for the increased formation of both amino acids. In line with this, we demonstrated that glycine, serine and cysteine were decreased in the *CNDP1*$^{-/-}$ mutants as well. Those three amino acids are interconnected in the metabolism by metabolic enzymes that are also found in human. Glycine and serine are precursors of each other, while serine can be further converted to cysteine [42, 55]. In addition to its known function in degrading carnosine, our data suggest a novel in vivo function for CN1 as regulator for the concentrations of specific amino acids in the metabolism. With the determination of the CN1 activity for Ala–His, Ser–His and His–Ala, we can already suggest Ser–His to be one of such dipeptides, as previously demonstrated for the recombinant enzyme [7]. This side activity of CN1 resembles to a certain degree the feature of metabolite repair enzymes like PM20D2, which was identified in mice and human to degrade dipeptide-byproducts that are synthesized by carnosine synthase CARNS [56]. Although further investigations need to be done to reveal the clearer function.

Moreover, we could show that CN2 is not affected by the knockout of *CNDP1*. Therefore, all observations are CN1-related and CN2 does not compensate for the loss of CN1. Yet, since the function of CN2 in zebrafish development, physiology and disease is unknown, its role must be determined in future experiments.

In the characterization of the zebrafish organ systems, the *CNDP1*$^{-/-}$ vasculature was not altered, but early embryonal pronephric structures showed some alterations, but they did not persist to adulthood. This implies that CN1, despite its involvement in amino acid metabolism, is not essential for normal organ development and physiology.

Despite the minor kidney alterations in *CNDP1*$^{-/-}$ embryos, *CNDP1*$^{-/-}$ mutants developed normal and reached adulthood. In the context of diabetic complications, we confirmed the recently published data from humans [20], showing that CN1 activity is modified, i.e., increased by MG similar as seen in diabetic mice. Yet, we have not seen beneficial effects of a *CNDP1* knockout, neither challenged by high MG levels nor by increased blood glucose, on kidney or vessel structures. It, therefore, seems likely, that the loss of CN1 and its respective increase in carnosine are not sufficient to protect against diabetic alterations in our knockout model. Although diabetic complications are not prevented, the increase in carnosine restrains weight gain to a certain degree, which indicates an anti-obesity effect of carnosine. However, the mechanism remained open since it could not be explained by an altered fatty acid and primary metabolite metabolism or dysregulation of blood glucose.

It should be kept in mind that several studies that reported beneficial effects of carnosine in diabetes models, administered carnosine in very high concentrations that naturally do not occur [18, 57, 58]. In obese Zucker rats dyslipidemia, body weight, and renal function were ameliorated under carnosine supplementation [59]. For humans, an additional supplementation of carnosine in the treatment of diabetes is considered to achieve the best outcome of the treatment as possible [60]. Clinical trials with simple carnosine supplementation could already show ameliorations of insulin resistance, fasting glucose, triglycerides, and glycation [61, 62]. However, our data also suggest that inhibition of CN1 activity alone as a therapeutic option is probably less promising because the increased concentration of carnosine by blocking CN1 activity does not reach therapeutically relevant concentrations. Thus, inhibition of CN1 activity and administration of carnosine together could be a promising strategy. This argument is underlined by a recent publication on the CN1 inhibitor carnostatine [23]. Carnostatine indeed effectively inhibited overexpressed human CN1 activity in mice and kept supplemented carnosine levels up, however, this study has not reported a diabetic animal model, where carnostatine and carnosine together improved diabetes induced organs alterations.

In conclusion, zebrafish exhibits carnosine and CN1 functions as other vertebrate model organisms. The knockout of *CNDP1* in zebrafish identified a novel function of CN1 in the amino acid metabolism. However, the knockout of *CNDP1* alone was not sufficient to protect from diabetic complications, but prevented profound weight gain.

Acknowledgements The study was supported by grants from Deutsche Forschungsgemeinschaft (CRC 1118 and IRTG 1874/2 DIAMICOM). We thank the Metabolomics Core Technology Platform of the Excellence cluster "CellNetworks" (University of Heidelberg) and the Deutsche Forschungsgemeinschaft (Grant ZUK 40/2010-3009262) for support with UPLC-based metabolite quantification. We acknowledge the support of the Core Facility Live Cell Imaging (DFG INST 91027/10-1 FUGG).

Author contributions FS: conceived and designed the analysis; data collection; contribution of data or analysis tools; performed the analysis (mutant generation, fish work, phenotyping of the mutants); wrote the paper; critical revision of the paper; data analysis and interpretation; final approval of the version to publish. VP: conceived and designed the analysis; data collection; contribution of data or analysis tools; performed the analysis (CN1 activity, carnosine and anserine determinations, western blot); critical revision of the paper; data analysis and interpretation; final approval of the version to publish. CPS: conceived and designed the analysis; contribution of data or analysis tools; critical revision of the paper; data analysis and interpretation; final approval of the version to publish. GP: data collection; contribution of data or analysis tools; performed the analysis (metabolomic analysis); critical revision of the paper; final approval of the version to publish. MB: data collection; contribution of data or analysis tools; performed the analysis (metabolomic analysis); critical revision of the paper; final approval of the version to publish. XL: data collection; contribution of data or analysis tools; performed the analysis (fish work); critical revision of the paper; final approval of the version to publish. TW: data collection; contribution of data or analysis tools'; performed the analysis (western blot); critical revision of the paper; final approval of the version to publish. TP: data collection; contribution of data or analysis tools; performed the analysis (analysis and quantification of adult fish kidneys); critical revision of the paper; final approval of the version to publish. NV: data collection; contribution of data or analysis tools; critical revision of the paper; final approval of the version to publish. JM: data collection; contribution of data or analysis tools; performed the analysis (methylglyoxal and glucose determintation); critical revision of the paper; final approval of the version to publish. TF: data collection; contribution of data or analysis tools; performed the analysis (methylglyoxal and glucose determintation); critical revision of the paper; final approval of the version to publish. PPN: conceived and designed the analysis; data collection; contribution of data or analysis tools; critical revision of the paper; final approval of the version to publish. JK: conceived and designed the analysis; contribution of data or analysis tools; critical revision of the paper; data analysis and interpretation; final approval of the version to publish.

Compliance with ethical standards

Conflict of interest The authors declare that they have no conflicts of interest with the contents of this article.

References

1. International Diabetes Federation (2017) IFD Diabetes Atlas, 8th edition
2. Lim AK (2014) Diabetic nephropathy—complications and treatment. Int J Nephrol Renovasc Dis 7:361–381
3. Doria A (1998) Genetic markers of increased susceptibility to diabetic nephropathy. Horm Res 50(Suppl 1):6–11
4. Mooyaart AL, Valk EJJ, Van Es LA et al (2011) Genetic associations in diabetic nephropathy: a meta-analysis. Diabetologia 54:544–553. https://doi.org/10.1007/s00125-010-1996-1
5. Boldyrev A, Aldini G, Derave W (2013) Physiology and pathophysiology of carnosine. Physiol Rev 93:1803–1845. https://doi.org/10.1152/physrev.00039.2012
6. Lenney JF, George RP, Weiss AM et al (1982) Human serum carnosinase: characterization, distinction from cellular carnosinase, and activation by cadmium. Clin Chim Acta 123:221–231. https://doi.org/10.1016/0009-8981(82)90166-8
7. Teufel M, Saudek V, Ledig JP et al (2003) Sequence identification and characterization of human carnosinase and a closely related non-specific dipeptidase. J Biol Chem 278:6521–6531. https://doi.org/10.1074/jbc.M209764200
8. Lenney JF (1976) Specifity and distribution of mammalian carnosinase. Biochem Biophys Acta 429:214–219
9. Peters V, Zschocke J, Schmitt CP (2018) Carnosinase, diabetes mellitus and the potential relevance of carnosinase deficiency. J Inherit Metab Dis 41:39–47. https://doi.org/10.1007/s10545-017-0099-2
10. Kalyankar G, Meister A (1959) Enzymatic synthesis of carnosine and related β-alanyl and γ-aminobutyryl peptides. J Biol Chem 234:3210–3218. https://doi.org/10.1016/j.tetasy.2009.05.040
11. Drozak J, Veiga-da-Cunha M, Vertommen D et al (2010) Molecular identification of carnosine synthase as ATP-grasp domain-containing protein 1 (ATPGD1). J Biol Chem 285:9346–9356. https://doi.org/10.1074/jbc.M109.095505
12. Vistoli G, Orioli M, Pedretti A et al (2009) Design, synthesis, and evaluation of carnosine derivatives as selective and efficient sequestering agents of cytotoxic reactive carbonyl species. ChemMedChem 4:967–975. https://doi.org/10.1002/cmdc.200800433
13. Hipkiss AR (2011) Energy metabolism, proteotoxic stress and age-related dysfunction—protection by carnosine. Mol Aspects Med 32:267–278. https://doi.org/10.1016/j.mam.2011.10.004
14. Alhamdani MSS, Al-Azzawie HF, Abbas FKH (2007) Decreased formation of advanced glycation end-products in peritoneal fluid by carnosine and related peptides. Perit Dial Int 27:86–89
15. Miceli V, Pampalone M, Frazziano G et al (2018) Carnosine protects pancreatic beta cells and islets against oxidative stress damage. Mol Cell Endocrinol 474:105–118. https://doi.org/10.1016/j.mce.2018.02.016
16. Sauerhöfer S, Yuan G, Braun GS et al (2007) L-carnosine, a substrate of carnosinase-1, influences glucose metabolism. Diabetes 56:2425–2432. https://doi.org/10.2337/db07-0177
17. Baye E, Ukropcova B, Ukropec J et al (2016) Physiological and therapeutic effects of carnosine on cardiometabolic risk and disease. Amino Acids 48:1131–1149. https://doi.org/10.1007/s00726-016-2208-1
18. Albrecht T, Schilperoort M, Zhang S et al (2017) Carnosine attenuates the development of both type 2 diabetes and diabetic nephropathy in BTBR ob/ob mice. Sci Rep 7:1–16. https://doi.org/10.1038/srep44492
19. Peters V, Riedl E, Braunagel M et al (2014) Carnosine treatment in combination with ACE inhibition in diabetic rats. Regul Pept 194–195:36–40. https://doi.org/10.1016/j.regpep.2014.09.005

20. Peters V, Lanthaler B, Amberger A et al (2015) Carnosine metabolism in diabetes is altered by reactive metabolites. Amino Acids 47:2367–2376. https://doi.org/10.1007/s00726-015-2024-z
21. Janssen B, Hohenadel D, Brinkkoetter P et al (2005) Carnosine as a protective factor in diabetic nephropathy: association with a leucine repeat of the carnosinase gene CNDP1. Diabetes 54:2320–2327. https://doi.org/10.2337/diabetes.54.8.2320
22. Senut M-C, Azher S, Margolis FL, Patei K, Mousa A, Majid A (2012) Distribution of carnosine-like peptides in the nervous system of developing and zebrafish (*Danio rerio*) and the embryonic effects of chronic carnosine exposure. Cell Tissue Res 29:997–1003. https://doi.org/10.1016/j.biotechadv.2011.08.021.Secreted
23. Qiu J, Hauske SJ, Zhang S et al (2018) Identification and characterisation of carnostatine (SAN9812), a potent and selective carnosinase (CN1) inhibitor with in vivo activity. Amino Acids. https://doi.org/10.1007/s00726-018-2601-z
24. Seth A, Stemple DL, Barroso I (2013) The emerging use of zebrafish to model metabolic disease. Dis Model Mech 6:1080–1088. https://doi.org/10.1242/dmm.011346
25. Heckler K, Kroll J (2017) Zebrafish as a model for the study of microvascular complications of diabetes and their mechanisms. Int J Mol Sci 18:1–9. https://doi.org/10.3390/ijms18092002
26. Perner B, Englert C, Bollig F (2007) The Wilms tumor genes wt1a and wt1b control different steps during formation of the zebrafish pronephros. Dev Biol 309:87–96. https://doi.org/10.1016/j.ydbio.2007.06.022
27. Lawson ND, Weinstein BM (2002) In vivo imaging of embryonic vascular development using transgenic zebrafish. Dev Biol 248:307–318. https://doi.org/10.1006/dbio.2002.0711
28. Kimmel C, Ballard W, Kimmel S et al (1995) Stages of embryonic development of the zebrafish. Dev Dyn 203:253–310
29. Sharma KR, Heckler K, Stoll SJ et al (2016) ELMO1 protects renal structure and ultrafiltration in kidney development and under diabetic conditions. Sci Rep 6:37172. https://doi.org/10.1038/srep37172
30. Jurczyk A, Roy N, Bajwa R et al (2011) Dynamic glucoregulation and mammalian-like responses to metabolic and developmental disruption in zebrafish. Gen Comp Endocrinol 170:334–345. https://doi.org/10.1016/j.ygcen.2010.10.010
31. Peters V, Klessens CQF, Baelde HJ et al (2015) Intrinsic carnosine metabolism in the human kidney. Amino Acids 47:2541–2550. https://doi.org/10.1007/s00726-015-2045-7
32. Jao L-E, Wente SR, Chen W (2013) Efficient multiplex biallelic zebrafish genome editing using a CRISPR nuclease system. Proc Natl Acad Sci USA 110:13904–13909. https://doi.org/10.1073/pnas.1308335110
33. Wiggenhauser LM, Kohl K, Dietrich N et al (2017) Studying diabetes through the eyes of a fish: microdissection, visualization, and analysis of the adult tg(fli:EGFP) zebrafish retinal vasculature. J Vis Exp. https://doi.org/10.3791/56674
34. Rueden CT, Schindelin J, Hiner MC et al (2017) Image J2: ImageJ for the next generation of scientific image data. BMC Bioinform 18:1–26. https://doi.org/10.1186/s12859-017-1934-z
35. Bürstenbinder K, Rzewuski G, Wirtz M et al (2007) The role of methionine recycling for ethylene synthesis in Arabidopsis. Plant J 49:238–249. https://doi.org/10.1111/j.1365-313X.2006.02942.x
36. Weger BD, Weger M, Görling B et al (2016) Extensive regulation of diurnal transcription and metabolism by glucocorticoids. PLoS Genet 12:1–24. https://doi.org/10.1371/journal.pgen.1006512
37. Wirtz M, Droux M, Hell R (2004) *O*-acetylserine (thiol) lyase: an enigmatic enzyme of plant cysteine biosynthesis revisited in *Arabidopsis thaliana*. J Exp Bot 55:1785–1798. https://doi.org/10.1093/jxb/erh201
38. Rabbani N, Thornalley PJ (2014) Measurement of methylglyoxal by stable isotopic dilution analysis LC–MS/MS with corroborative prediction in physiological samples. Nat Protoc 9:1969
39. Oka T, Nishimura Y, Zang L et al (2010) Diet-induced obesity in zebrafish shares common pathophysiological pathways with mammalian obesity. BMC Physiol 10:21. https://doi.org/10.1186/1472-6793-10-21
40. Wilkinson RN, van Eeden FJM (2014) The zebrafish as a model of vascular development and disease. Prog Mol Biol Transl Sci 124:93–122. https://doi.org/10.1016/B978-0-12-386930-2.00005-7
41. Amelio I, Cutruzzolá F, Antonov A et al (2014) Serine and glycine metabolism in cancer. Trends Biochem Sci 39:191–198. https://doi.org/10.1016/j.tibs.2014.02.004
42. Kalhan SC, Hanson RW (2012) Resurgence of serine: an often neglected but indispensable amino acid. J Biol Chem 287:19786–19791. https://doi.org/10.1074/jbc.R112.357194
43. Jackson MC, Kucera CM, Lenney JF (1991) Purification and properties of human serum carnosinase. Clin Chim Acta 196:193–205
44. Brownlee M (2001) Biology of diabetic complications. Nature 414:813–820. https://doi.org/10.1038/414813a
45. Lo TWC, Westwood ME, McLellan AC et al (1994) Binding and modification of proteins by methylglyoxal under physiological conditions: a kinetic and mechanistic study with Nα-acetylarginine, Nα-acetylcysteine, and Nα-acetyllysine, and bovine serum albumin. J Biol Chem 269:32299–32305
46. Jörgens K, Stoll SJ, Pohl J et al (2015) High tissue glucose alters intersomitic blood vessels in zebra fish via methylglyoxal targeting the VEGF receptor signaling cascade. Diabetes 64:213–225. https://doi.org/10.2337/db14-0352
47. Kimmel RA, Onder L, Wilfinger A et al (2011) Requirement for Pdx1 in specification of latent endocrine progenitors in zebrafish. BMC Biol 9:75. https://doi.org/10.1186/1741-7007-9-75
48. Song BC, Joo N-S, Aldini G, Yeum K-J (2014) Biological functions of histidine-dipeptides and metabolic syndrome. Nutr Res Pract 8:3. https://doi.org/10.4162/nrp.2014.8.1.3
49. Baye E, Ukropec J, De Courten MP et al (2017) Effect of carnosine supplementation on the plasma lipidome in overweight and obese adults: a pilot randomised controlled trial. Sci Rep 7:1–7. https://doi.org/10.1038/s41598-017-17577-7
50. Peters V, Kebbewar M, Jansen EW et al (2010) Relevance of allosteric conformations and homocarnosine concentration on carnosinase activity. Amino Acids 38:1607–1615. https://doi.org/10.1007/s00726-009-0367-z
51. Bando K, Shimotsuji T, Toyoshima H et al (1984) Fluorometric assay of human serum carnosinase activity in normal children, adults and patients with myopathy. Ann Clin Biochem 21(Pt 6):510–514. https://doi.org/10.1177/000456328402100613
52. Peñafiel R, Ruzafa C, Monserrat F, Cremades A (2004) Gender-related differences in carnosine, anserine and lysine content of murine skeletal muscle. Amino Acids 26:53–58. https://doi.org/10.1007/s00726-003-0034-8
53. Kohen R, Yamamoto Y, Cundy KC, Ames BN (1988) Antioxidant activity of carnosine, homocarnosine, and anserine present in muscle and brain. Proc Natl Acad Sci 85:3175–3179. https://doi.org/10.1073/pnas.85.9.3175
54. Peters V, Calabrese V, Forsberg E et al (2018) Protective actions of anserine under diabetic conditions. Int J Mol Sci 19:2751. https://doi.org/10.3390/ijms19092751
55. Van De Poll MCG, Soeters PB, Deutz NEP et al (2004) Renal metabolism of amino acids: its role in interorgan amino acid exchange. Am J Clin Nutr 79:185–197. https://doi.org/10.1093/ajcn/79.2.185
56. Veiga-da-Cunha M, Chevalier N, Stroobant V et al (2014) Metabolite proofreading in carnosine and homocarnosine synthesis: molecular identification of PM20D2 as β-alanyl-lysine dipeptidase. J Biol Chem 289:19726–19736. https://doi.org/10.1074/jbc.M114.576579

57. Lee YT, Hsu CC, Lin MH et al (2005) Histidine and carnosine delay diabetic deterioration in mice and protect human low density lipoprotein against oxidation and glycation. Eur J Pharmacol 513:145–150. https://doi.org/10.1016/j.ejphar.2005.02.010
58. Pfister F, Riedl E, Wang Q et al (2011) Oral carnosine supplementation prevents vascular damage in experimental diabetic retinopathy. Cell Physiol Biochem 28:125–136. https://doi.org/10.1159/000331721
59. Aldini G, Orioli M, Rossoni G et al (2011) The carbonyl scavenger carnosine ameliorates dyslipidaemia and renal function in Zucker obese rats. J Cell Mol Med 15:1339–1354. https://doi.org/10.1111/j.1582-4934.2010.01101.x
60. Everaert I, Taes Y, De Heer E et al (2012) Low plasma carnosinase activity promotes carnosinemia after carnosine ingestion in humans. AJP Ren Physiol 302:F1537–F1544. https://doi.org/10.1152/ajprenal.00084.2012
61. De Courten B, Jakubova M, De Courten MPJ et al (2016) Effects of carnosine supplementation on glucose metabolism: pilot clinical trial. Obesity 24:1027–1034. https://doi.org/10.1002/oby.21434
62. Houjeghani S, Kheirouri S, Faraji E, Jafarabadi MA (2018) L-Carnosine supplementation attenuated fasting glucose, triglycerides, advanced glycation end products, and tumor necrosis factor–α levels in patients with type 2 diabetes: a double-blind placebo-controlled randomized clinical trial. Nutr Res 49:96–106

Affiliations

Felix Schmöhl[1] · Verena Peters[2] · Claus Peter Schmitt[2] · Gernot Poschet[3] · Michael Büttner[3] · Xiaogang Li[1] · Tim Weigand[2] · Tanja Poth[4] · Nadine Volk[5] · Jakob Morgenstern[6] · Thomas Fleming[6] · Peter P. Nawroth[6,7,8] · Jens Kroll[1]

Felix Schmöhl
felix.schmoehl@gmail.com

Verena Peters
verena.peters@med.uni-heidelberg.de

Claus Peter Schmitt
clauspeter.schmitt@med.uni-heidelberg.de

Gernot Poschet
gernot.poschet@cos.uni-heidelberg.de

Michael Büttner
michael.buettner@cos.uni-heidelberg.de

Xiaogang Li
xiaogang.li@medma.uni-heidelberg.de

Tim Weigand
tim.weigand@med.uni-heidelberg.de

Tanja Poth
tanja.poth@med.uni-heidelberg.de

Nadine Volk
nadine.volk@med.uni-heidelberg.de

Jakob Morgenstern
jakob.morgenstern@med.uni-heidelberg.de

Thomas Fleming
thomas.fleming@med.uni-heidelberg.de

Peter P. Nawroth
peter.nawroth@med.uni-heidelberg.de

[1] European Center for Angioscience (ECAS), Department of Vascular Biology and Tumor Angiogenesis, Medical Faculty Mannheim, Heidelberg University, Ludolf-Krehl-Str. 13-17, 68167 Mannheim, Germany

[2] Center for Paediatric and Adolescent Medicine, University of Heidelberg, Im Neuenheimer Feld 669, 69120 Heidelberg, Germany

[3] Center for Organismal Studies (COS), University of Heidelberg, Im Neuenheimer Feld 360, 69120 Heidelberg, Germany

[4] CMCP-Center for Model System and Comparative Pathology, Institute of Pathology, University Hospital Heidelberg, Im Neuenheimer Feld 224, 69120 Heidelberg, Germany

[5] Tissue Bank of the National Center for Tumor Diseases (NCT), Im Neuenheimer Feld 224, 69120 Heidelberg, Germany

[6] Department of Internal Medicine I and Clinical Chemistry, Heidelberg University Hospital, Im Neuenheimer Feld 410, 69120 Heidelberg, Germany

[7] German Center for Diabetes Research (DZD), 85764 München-Neuherberg, Germany

[8] Joint Heidelberg-IDC Translational Diabetes Program, Helmholtz-Zentrum, München, Im Neuenheimer Feld 410, F02 Room 02.414-02.434, 69120 Heidelberg, Germany